Radar signal enhancement using feasible direction methods

M G Selim[1*], G Mabrouk[1], A K Elsherif[1] and A Youssef[2]

[1] Engineering Mathematics Department, Military Technical College, Cairo, Egypt.
[2] Radar Department, Military Technical College, Cairo, Egypt.

[*]E-mail: mohamed.gamal@mtc.edu.eg

Abstract. Conventional radars have made extensive use of the linear frequency modulated (LFM) signals. Nevertheless, its radar detectability is negatively impacted by its high sidelobe level (SLL). Modern radars use nonlinear frequency modulated (NLFM) signals to overcome the masking problem by obtaining suppressed sidelobes of radar matching filter output while preserving the mainlobe level and resolution. In this paper, NLFM signals are optimized to get very low SLL while maintaining the mainlobe width (MLW) and hence improving range resolution and radar detection capabilities. An optimization framework will be introduced depending mainly on feasible direction methods which move towards the optimal solution iteratively within the feasible region to optimize the proposed NLFM signal that is generated by an instantaneous frequency function described by tan function. This framework relies on two nonlinear optimization techniques that are Zoutendijk's method of feasible directions (ZMFD) and Rosen's gradient projection method (RGPM). These methods solve the nonlinear optimization issue by advancing in the feasible search direction from a feasible point to an enhanced feasible one. Simulation results of the autocorrelation function (ACF) of the optimized NLFM signal reveal its superiority in suppressing SLL compared to LFM signal and preserving MLW of the radar signal. The detailed mathematical description of these two algorithms is also included in this work. Furthermore, two metrics are also calculated to ensure the quality of the resulted signals which are the impulse response width (IRW) and integrated sidelobe ratio (ISLR). Finally, all these results are tabulated to compare the two optimization techniques and the radar designers should choose the best technique depending on the radar system application.

Keywords: nonlinear optimization, nonlinear frequency modulated signal, sidelobe level, mainlobe width, autocorrelation function, radar waveform optimization, feasible direction methods, Zoutendijk's method of feasible directions, Rosen's gradient projection method.

1. Introduction

The issue of target masking in a radar waveform array is tackled by low-sidelobe radar signals, thereby raising the probability of inadequate target detection [1]. In order to attain low sidelobe level (SLL), nonlinear frequency modulated (NLFM) waveforms may have an S-shaped time frequency function. But with NLFM waveforms, the signal-to-noise ratio is not adversely affected, and the mainlobe width (MLW) broadens [2]. As a result, pulse compression techniques specially NLFM ones, are widely used in modern radar systems. Several optimization strategies could be used to further improve these kinds of signals and enhance its characteristics such as suppressing SLL and maintain MLW. These techniques could be bioinspired inspired, physically inspired or swarm intelligence techniques [3].

One of these techniques is the Lagrangian method that was used to reduce the sidelobes of a NLFM signal results in an enhanced one by around 5 dB SLL compared with the stationary phase method [4]. Genetic algorithm (GA) was also applied to improve SLL performance resulting in an enhanced nonlinear chirp with -28.01 dB SLL [5]. In [6], a mathematical model waveform design was established which expressed the instantaneous frequency as combination of a sine series and a linear function. The optimal parameters of this signal had been evaluated using simulated annealing algorithm that achieves a peak sidelobe ratio (PSLR) below -60 dB. Blunt et al. [7] applied the nonlinear conjugate gradient descent algorithm to optimize the parameters of polyphase-coded FM (PCFM) radar waveforms which resulted in an enhanced waveform with -52 dB SLL. Ling-jin et al. [8] combined the cyclic algorithm (CA) with the convex optimization (CO) and investigated a new model targeting a flexible trade-off between sidelobe suppression and mainlobe widening that was feasible to meet the requirements of different target detection scenarios achieving PSLR under -55 dB. The sequential quadratic programming technique and the interior point method were applied in weather radars in order to get minimum sidelobe energy and peak level through a strategy based on nonlinear iterative optimization [9]. Walsh matrix and GA are used in [10] to generate executing orthogonal biphase-coded signals with low auto-correlation sidelobe peak and cross-correlation peak, resulting in more precise results. Avishek [11] used two stochastic optimization methods, the social spider algorithm (SSA) and the modified social spider algorithm (MSSA) to optimize the far-field radiation pattern of a concentric circular antenna array (CCAA) design by suppressing SLL. Many evolutionary optimization techniques are used to suppress SLL of the antenna array such as cuckoo search algorithm, the particle swarm optimization, the fruitfly optimization algorithm, the ant colony optimization algorithm and dragonfly algorithm [12,13]. In this article, two feasible direction methods such as Zoutendijk's method and Rosen's gradient projection method are used to optimize the coefficients of the proposed NLFM signal [14].

The remainder of this paper is organized as follows. In Section 2, the mathematical derivation of the proposed problem is introduced. Section 3 gives a brief overview of the feasible direction methods and how they are used to solve nonlinear optimization problems. In Section 4, the feasible direction method of Zoutendijk is illustrated with its mathematical description. In Section 5, the simulation results of Zoutendijk's method are given. In Section 6, the gradient projection method of Rosen is discussed with its detailed mathematical derivation. Section 7 presents the results of Rosen's method with its simulated ACF. In Section 8, the discussion of the results is introduced. Finally, the conclusion and the future work are given in Section 9.

2. Mathematical derivation of the problem

The instantaneous frequency function of the proposed NLFM signal is defined as [15]:

$$f_I(t) = k_1.B.tan\left(\frac{k_2.t}{T}\right) \quad \#(1)$$

where k_1, k_2 are the coefficients needed to be optimized and B is the bandwidth of the pulse, while T is the pulse duration. The relation between the instantaneous frequency and the phase is given by [16]:

$$f_I(t) = \frac{1}{2}\frac{d\Phi(t)}{dt} \qquad \#(2)$$

Integrating equation (1) and substituting in equation (2) gives the relation of the corresponding phase of the NLFM signal which is expressed as follows:

$$\Phi(t) = -2\pi \cdot \frac{k_1}{k_2} \cdot BT \cdot In\left(\left|cos\left(\frac{k_2.t}{T}\right)\right|\right) \qquad \#(3)$$

The transmitted NLFM signal is given by:

$$x(t) = b(t).e^{j\Phi(t)} = b(t).e^{j\left(-2\pi\cdot\frac{k_1}{k_2}\cdot BT\cdot In\left(\left|cos\left(\frac{k_2.t}{T}\right)\right|\right)\right)} \qquad \#(4)$$

where $b(t)$ is the amplitude of the signal.

The ACF of the NLFM signal is defined as [12]:

$$g(t) = \int_{-\infty}^{\infty} x(\tau)x^*(\tau + t)d\tau \qquad \#(5)$$

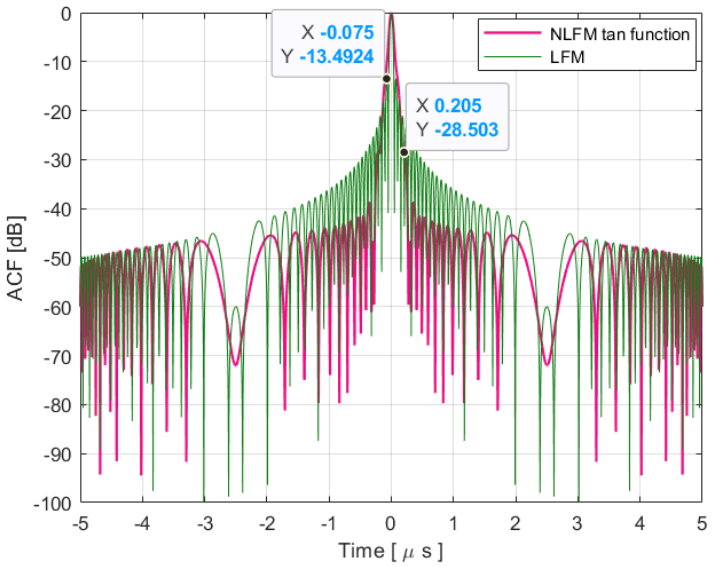

Figure 1. ACFs of LFM and NLFM signals.

Figure 1 shows the ACF of the NLFM tan signal compared to that of the LFM one. It is clear that the LFM signal has narrower MLW but higher SLL around -13.4924 dB. On the other hand, NLFM one has lower SLL of almost -28.503 dB, but it exhibits wider mainlobe. The NLFM signal obviously has a reduced SLL, which improves radar detectability and range resolution.

The aim is to create a transmitted pulse that has certain characteristics of its ACF, resulting in a highly peaked function with the narrowest possible mainlobe and the lowest possible sidelobe. Because of the conflict between these features, a trade-off should be established during the

design process. In this paper, the mainlobe width is represented by the design parameter ω which is controlled by the constant б and connected to the bandwidth B through the relation $\omega = \frac{2*б}{B}$ in which б ≥ 1. The previous relation results in the MLW of LFM signal in case of б = 1. The signal sidelobes which exist in the two intervals $L_n^+ = [\omega/2, T]$ and $L_n^- = [-T, -\omega/2]$ ought to hold the lowest amount of energy of $g(t)$ while the mainlobe that exists in the interval $L_m = [-\omega/2, \omega/2\ ]$, ought to hold the highest amount of energy of $g(t)$ [16].

Suppose that Ω_n is the set of indices n such that $t_n \in [-T, -\omega/2] \cup [\omega/2, T] = L_n^- \cup L_n^+$. Also, suppose that Ω_m is the set of indices m so that $t_m \in [-\omega/2, \omega/2\ ] = L_m$ i.e., $\Omega_s = \Omega_m + \Omega_n$ in which Ω_s denotes the whole NLFM signal. The main goal is to decrease the sidelobes energy which could be expressed as:

$$E(t) = \sum_{n \in \Omega_n} |g(t_n)|^2 \qquad \#(6)$$

whereas maintaining the mainlobe energy unaffected as much as possible and it could be determined by the following relation:

$$c(t) = \sum_{m \in \Omega_m} |g(t_m)|^2 \quad \#(7)$$

To ascertain this, a vector of constants **k** given by $[k_1 \ \ k_2]$ is proposed and the objective is to evaluate the optimum values of **k** that results in the narrower MLW and the minimum SLL. The formulation will start with finding the formula for the energy of sidelobes. Substituting equation (5) into equation (6) results in:

$$E(t) = \sum_{n \in \Omega_n} \int_{-\infty}^{\infty} x(\tau) x^*(\tau + t) d\tau \qquad \#(8)$$

then, by substitution of equation (4) into equation (8) results that:

$$E(t) = \sum_{n \in \Omega_n} \left| \int_{-\infty}^{\infty} b(t).\, e^{-j\left(2\pi \cdot \frac{k_1}{k_2} \cdot BT \cdot \ln\left(\left|\cos\left(\frac{k_2 \cdot \tau}{T}\right)\right|\right)\right)} b(t) \cdot e^{j\left(2\pi \cdot \frac{k_1}{k_2} \cdot BT \cdot \ln\left(\left|\cos\left(\frac{k_2 \cdot (\tau + t_n)}{T}\right)\right|\right)\right)} d\tau \right|^2 \qquad \#(9)$$

$$E(t) = \sum_{n \in \Omega_n} \left| \int_{-\infty}^{\infty} b^2(t) \cdot e^{\left(-j\left(2\pi \cdot \frac{k_1}{k_2} \cdot BT \cdot \ln\left(\left|\cos\left(\frac{k_2 \cdot \tau}{T}\right)\right|\right)\right) + j\left(2\pi \cdot \frac{k_1}{k_2} \cdot BT \cdot \ln\left(\left|\cos\left(\frac{k_2 \cdot (\tau + t_n)}{T}\right)\right|\right)\right)\right)} d\tau \right|^2 \qquad \#(10)$$

Simplifying equation (10) yields that:

$$E(t) = \sum_{n \in \Omega_n} \left| \int_{-\infty}^{\infty} b^2(t).\, e^{j2\pi \cdot \frac{k_1}{k_2} \cdot BT \left(\ln\left(\left|\cos\left(\frac{k_2(\tau + t_n)}{T}\right)\right|\right) - \ln\left(\left|\cos\left(\frac{k_2 \tau}{T}\right)\right|\right)\right)} d\tau \right|^2 \qquad \#(11)$$

Hence, and depending on previous assumptions, equation (12) could be regarded as the cost function of the mathematical model that needed to be minimized. The constraint of that mathematical model is to keep the energy of the mainlobe constant as possible. By analogy, and depending on the previous derivation of the sidelobes energy, the mainlobe energy could be expressed as follows:

$$c(t) = \sum_{m\in\Omega_m} \left| \int_{-\infty}^{\infty} b^2(t).\, e^{j2\pi\cdot\frac{k_1}{k_2}\cdot BT\left(\ln\left(\left|\cos\left(\frac{k_2(\tau+t_m)}{T}\right)\right|\right)-\ln\left(\left|\cos\left(\frac{k_2\tau}{T}\right)\right|\right)\right)} d\tau \right|^2 \quad \#(12)$$

The LFM signal has been taken as a reference to the constraint on the mainlobe. From the previous assumptions, the model of the proposed optimization problem could be formulated as:

$$minimize_{\mathbf{b}} \;\; E(t) = \sum_{n\in\Omega_n} \left| \int_{-\infty}^{\infty} b^2(t).\, e^{j2\pi\cdot\frac{k_1}{k_2}\cdot BT\left(\ln\left(\left|\cos\left(\frac{k_2(\tau+t_n)}{T}\right)\right|\right)-\ln\left(\left|\cos\left(\frac{k_2\tau}{T}\right)\right|\right)\right)} d\tau \right|^2$$

$$subject\ to: \;\; c(t) = \sum_{m\in\Omega_m} \left| \int_{-\infty}^{\infty} b^2(t).\, e^{j2\pi\cdot\frac{k_1}{k_2}\cdot BT\left(\ln\left(\left|\cos\left(\frac{k_2(\tau+t_m)}{T}\right)\right|\right)-\ln\left(\left|\cos\left(\frac{k_2\tau}{T}\right)\right|\right)\right)} d\tau \right|^2 - \frac{2}{B} \leq \mathbf{0} \#(13)$$

Now, the previous problem will be solved using feasible direction methods, as described next.

3. Feasible direction methods (FDMs) for solving nonlinear optimization problems

Constrained optimization problems have a major challenge that is to search the solution space while ensuring that the identified solutions fulfil the imposed constraints as shown in figure 2. This difficulty is addressed by FDMs, which move towards the optimal solution iteratively within the feasible region. These methods solve the nonlinear optimization issue by advancing from a feasible point to an enhanced feasible one.

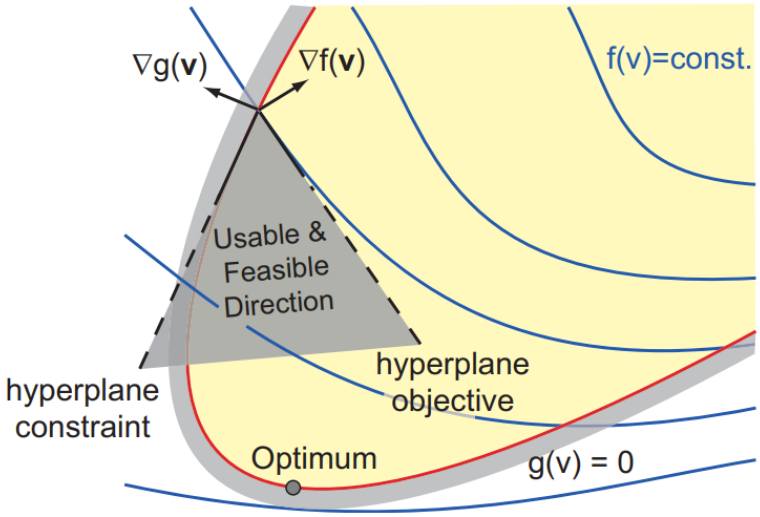

Figure 2. Illustration of method of feasible directions [17].

Since Zoutendijk developed the theory and the basis of FDMs in the 1960s, several basic modifications and adaptations of FDMs have been investigated and presented [18]. These methods have a lot of advantages such as high efficiency in solving nonlinear optimization issues, faster convergence and higher implementation simplicity.

In that approach, we select a starting point fulfilling all the constraints and proceed to an improved point depending on a suitable iteration $\mathbf{T}_{i+1} = \mathbf{T}_i + \lambda_i \mathbf{S}_i$ where $\mathbf{S}_i$ is the movement direction, $\mathbf{T}_i$ is the start point for the i^{th} iteration, $\mathbf{T}_{i+1}$ is the final point reached after the iteration i ended and λ is the step length. The search direction $\mathbf{S}_i$ is detected so that no constraint is violated by the motion in that direction and the objective function value could be minimized in

this direction. The step length λ is selected such that the point $\mathbf{T}_{i+1}$ is located inside the feasible region. The next iteration starts by $\mathbf{T}_{i+1}$ then the whole procedures is repeated until it reaches the point at which no direction satisfying both previous conditions can be determined [14]. The procedures for feasible direction methods are shown in figure 3.

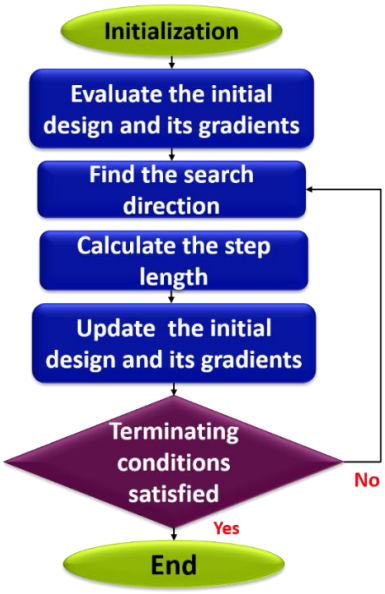

Figure 3. Procedures for feasible direction methods.

4. Feasible direction method of Zoutendijk

In this method, Zoutendijk stated that if the initial point of the iteration is inside the feasible region, then the usable feasible direction is regarded as the negative direction of the gradient. If the initial point is on the feasible region's boundary, some of the constraints become active, and the usable feasible direction is identified by satisfying the following equations:

$$\frac{d}{d\lambda} E(\mathbf{T}_i + \lambda \mathbf{S})\Big|_{\lambda=0} = \mathbf{S}^{\mathrm{T}} \nabla E(\mathbf{T}_i) < 0$$

$$\frac{d}{d\lambda} c_j(\mathbf{T}_i + \lambda \mathbf{S})\Big|_{\lambda=0} = \mathbf{S}^{\mathrm{T}} \nabla c_j(\mathbf{T}_i) \leq 0 \#(14)$$

When using this approach, there are various factors to consider. The first one is determining an appropriate usable feasible direction (S), the second one is finding an appropriate step size along the path S and the last one is the termination criterion [14]. All of these factors are illustrated further below.

4.1 Step length determination

There are several methods for determining the optimum value of the step length λ_i which reduces $f(\boldsymbol{T}_i + \lambda \boldsymbol{S}_i)$ so that the next point $\boldsymbol{T}_{i+1} = \boldsymbol{T}_i + \lambda_i \boldsymbol{S}_i$ is inside the feasible region. These methods are the bisection method, the Fibonacci method, the golden section search or the Newton method. The new point has three cases as follows:

- If $\boldsymbol{T}_{i+1}$ lies **inside** the feasible region, no active constraint is found hence the new usable feasible direction is expressed as $\boldsymbol{S}_{i+1} = -\nabla \mathrm{E}\ (\boldsymbol{T}_{i+1})$ and the technique proceeds to the new iteration.

- If $\boldsymbol{T}_{i+1}$ is **on** the feasible region's boundary, a new direction-finding problem is solved in order to find a new feasible direction S = $\boldsymbol{S}_{i+1}$.
- If $\boldsymbol{T}_{i+1}$ lies **outside** the feasible region, then λ_i has to be minimized so that the new point is inside the feasible region.

4.2 Direction finding problem

If $\boldsymbol{T}_i$ is inside the feasible region [i.e., $\nabla c_j\,(\boldsymbol{T}_i) < 0 \;\; \forall \;\; j = 1, 2, 3, \ldots, k$], the usable feasible direction could be expressed as:

$$\boldsymbol{S}_i = -\nabla E(\boldsymbol{T}_i) \qquad \#(15)$$

When some of the constraints become active i.e., $\nabla c_j\,(\boldsymbol{T}_i) = 0$, the problem becomes more complex. In this case, there is a simple approach to determine the usable feasible direction at $\boldsymbol{T}_i$ by generating a vector randomly such that it satisfies equation (15). So, the main goal is to find a feasible direction that minimizes the objective function and in addition directs away from the active constraints. This could be achieved by solving the following problem:

$$\begin{aligned} &max && \alpha \\ &subject\ to && \boldsymbol{S}^T \nabla c_j(\boldsymbol{T}_i) + p_j \alpha \le 0\,, \quad j \in J \\ & && \boldsymbol{S}^T \nabla E(\boldsymbol{T}_i) + \alpha \le 0\,, \qquad i = 1, 2, 3, \ldots, n \end{aligned} \qquad \#(16)$$

where α is an additional design variable, $\boldsymbol{J}$ is the active constraint set and p_j are arbitrarily non negative scalar constants and for simplicity set $p_j = 1$.

4.3 Termination criterion

The algorithm terminates when the optimization procedure converges and the following two conditions are satisfied in the current iteration:

$$\left| \frac{E(\mathbf{T}_i) - E(\mathbf{T}_{i+1})}{E(\mathbf{T}_i)} \right| \le \varepsilon_2 \quad \text{and} \quad \|\mathbf{T}_i - \mathbf{T}_{i+1}\| \le \varepsilon_3 \qquad \#(17)$$

where ε_2 and ε_3 are very small tolerances set for convergence of the algorithm [19]. Now the feasible direction method of Zoutendijk could be summarized as shown in algorithm 1.

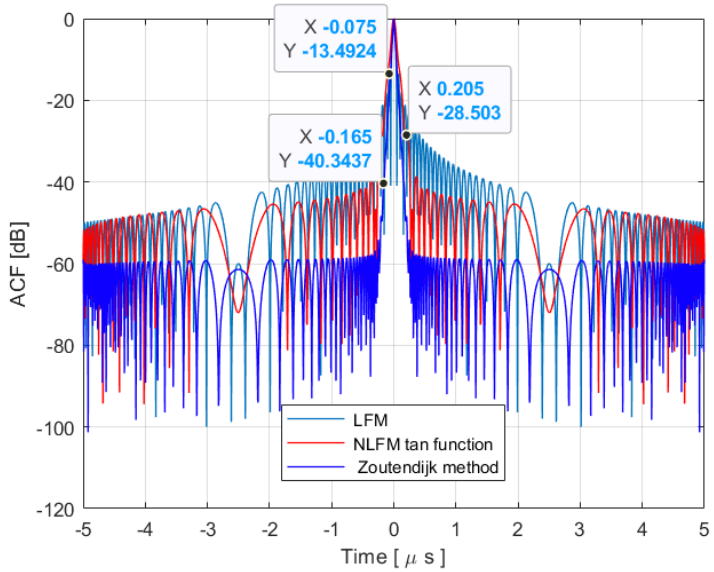

Figure 4. ACF of the signal optimized by Zoutendijk method compared to that of the original non-optimized tan signal and LFM signal.

5. Simulation results of Zoutendijk's method of feasible directions

The ACF of the NLFM signal optimized by the feasible direction method of Zoutendijk is shown in figure 4. As shown, the ACF of the optimized signal has SLL below -40 dB and MLW of 0.0673 μs. This method reduces the SLL by 12 dB and the other remaining sidelobes converge asymptotically to -60 dB. Also, it enhances the MLW by almost 0.0278 μs compared to the reference signal.

Table 1. Feasible direction method of Zoutendijk.

	Algorithm 1. Feasible direction method of Zoutendijk [14].
1	Initialize the feasible point $\mathbf{T}_1$ and the tolerances $\varepsilon_1, \varepsilon_2$, and ε_3 then evaluate $E(\mathbf{T}_1)$ and $c_j(\mathbf{T}_1)$ and set $i = 1$.
2	If $c_j(\mathbf{T}_i) < 0$ and $j = 1,2,3, \dots, m$, set $\mathbf{S}_i = -\nabla E(\mathbf{T}_i)$ then normalize $\mathbf{S}_i$ and go to step 5 of the algorithm. else $\left(c_j(\mathbf{T}_i) = 0\right)$, go to step 4 of the algorithm.
3	End if.
4	Solve the following problem to find an appropriate usable feasible direction $\mathbf{S}$ $$\begin{aligned} &min && -\alpha \\ &\text{s. t.} && \mathbf{S}^{\mathrm{T}}\nabla_{c_j}(\mathbf{T}_i) + p_j\alpha \le 0, \quad j = 1,2, \dots, m \\ & && \boldsymbol{S}^{\mathrm{T}}\nabla E + \alpha \le 0 \\ & && -1 \le s_i \le 1, \quad i = 1,2, \dots, n \end{aligned}$$
5	If the value of $\alpha^* \simeq 0 \le \varepsilon_1$, terminate the computation with $\mathbf{T}_{\text{opt}} \simeq \mathbf{T}_i$. else $(\alpha^* > \varepsilon_1)$, go to step 7 of the algorithm by setting $\mathbf{S}_i = \mathbf{S}$.
6	End if.
7	Determine an appropriate step length λ_i across $\mathbf{S}_i$ and evaluate $\mathbf{T}_{i+1}$ as $\mathbf{T}_{i+1} = \mathbf{T}_i + \lambda_i\mathbf{S}_i$.
8	Measure the cost function $E(\mathbf{T}_{i+1})$ then test the convergence of the method as in step 9 of the algorithm.
9	If $\left\lvert\frac{E(\mathbf{T}_i)-E(\mathbf{T}_{i+1})}{E(\mathbf{T}_i)}\right\rvert \le \varepsilon_2$ and $\lVert\mathbf{T}_i - \mathbf{T}_{i+1}\rVert \le \varepsilon_3$ terminate with $\mathbf{T}_{\text{opt}} \simeq \mathbf{T}_{i+1}$. else go to step 10.
10	Set $i = i + 1$ to proceed to the new iteration, and repeat the entire process.

6. The gradient projection method of Rosen

In this method, Rosen used the projection of the negative gradient of the objective function onto the active constraints and stated that the usable feasible direction is determined without solving any auxiliary linear optimization problem. Consider the following problem:

$$\begin{aligned} &\min \quad E(\mathbf{T}) \\ &\text{s.t.} \quad c_j(\mathbf{T}) \le 0 \quad \forall \quad j = 1,2,3, \dots, m \end{aligned} \qquad \#(18)$$

Let $j_1, j_2, \dots, j_r$ be the set of active constraint indices at any point and $\nabla c_j(\mathbf{T})$ be the active constraint gradients. The matrix $\mathbf{N}$ with order $n \times r$ is defined as follows:

$$\mathbf{N} = \left[\nabla c_{j1} \nabla c_{j2} \dots \nabla c_{jr}\right] \qquad \#(19)$$

where n denotes the number of variables, then the proposed usable feasible direction S could be obtained by solving the following optimization problem:

$$\begin{aligned} min \quad & \mathbf{S}^T \nabla E(\mathbf{T}) \\ \text{s.t.} \quad & \mathbf{N}^T \mathbf{S} = 0 \\ & \mathbf{S}^T \mathbf{S} - 1 = 0 \end{aligned} \qquad \#(20)$$

in which $\mathbf{S}^T \mathbf{S} - 1 = 0$ indicates the normalization of $\mathbf{S}$.
The Lagrangian function of this equality-constrained problem could be constructed as follow:

$$L(\mathbf{S}, \lambda, \beta) = \lambda^{\mathrm{T}} \mathbf{N}^{\mathrm{T}} \mathbf{S} + \beta\left(\mathbf{S}^{\mathrm{T}} \mathbf{S} - 1\right) + \mathbf{S}^{\mathrm{T}} \nabla E(\mathbf{T}) \qquad \#(21)$$

where β is the Lagrange multiplier of the first constraint in equation (21) and λ is the Lagrange multipliers vector of the second constraint in equation (21) and it is expressed as:

$$\lambda = \begin{Bmatrix} \lambda_1 \\ \lambda_2 \\ \vdots \\ \lambda_r \end{Bmatrix} \qquad \#(22)$$

The partial derivatives of L w.r.t. $\mathbf{S}$, λ and β represent the necessary conditions for the minimum and they are given by:

$$\begin{aligned} \frac{\partial L}{\partial \mathbf{S}} &= \nabla E(\mathbf{T}) + \mathbf{N}\lambda + 2\beta \mathbf{S} = \mathbf{0} \\ \frac{\partial L}{\partial \lambda} &= \mathbf{N}^{\mathrm{T}} \mathbf{S} = \mathbf{0} \\ \frac{\partial L}{\partial \beta} &= \mathbf{S}^{\mathrm{T}} \mathbf{S} - 1 = 0 \end{aligned} \qquad \#(23)$$

From the first equation in equation (24), $\mathbf{S}$ could be expressed as:

$$\mathbf{S} = -\frac{1}{2\beta}\left(\nabla E(\mathbf{T}) + \mathbf{N}\lambda\right) \qquad \#(24)$$

By substituting equation (25) into the second equation in equation (24) gives:

$$\mathbf{N}^{\mathrm{T}} \mathbf{S} = -\frac{1}{2\beta}\left(\mathbf{N}^{\mathrm{T}} \nabla E(\mathbf{T}) + \mathbf{N}^{\mathrm{T}} \mathbf{N}\lambda\right) = \mathbf{0}, \qquad \#(25)$$

which could be expressed as:

$$\mathbf{N}^{\mathrm{T}} \nabla E(\mathbf{T}) + \mathbf{N}^{\mathrm{T}} \mathbf{N}\lambda = \mathbf{0} \qquad \#(26)$$

from which λ can be found as:

$$\lambda = -\left(\mathbf{N}^{\mathrm{T}} \mathbf{N}\right)^{-1} \mathbf{N}^{\mathrm{T}} \nabla E(\mathbf{T}) \qquad \#(27)$$

Substituting λ into equation (25) gives

$$\mathbf{S} = -\frac{1}{2\beta}\left(\mathbf{I} - \mathbf{N}\left(\mathbf{N}^{\mathrm{T}} \mathbf{N}\right)^{-1} \mathbf{N}^{\mathrm{T}}\right) \nabla E(\mathbf{T}) = -\frac{1}{2\beta} \mathbf{P} \nabla E(\mathbf{T}) \qquad \#(28)$$

where $\mathbf{P}$ is defined as the projection matrix and it is expressed as:

$$\mathbf{P} = \mathbf{I} - \mathbf{N}\left(\mathbf{N}^{\mathrm{T}} \mathbf{N}\right)^{-1} \mathbf{N}^{\mathrm{T}} \qquad \#(29)$$

The vector $\mathbf{S}$ could be normalized according to the next equation:

$$\mathbf{S} = -\frac{\mathbf{P}\nabla E(\mathbf{T})}{\| \mathbf{P}\nabla E(\mathbf{T}) \|} \qquad \#(30)$$

Starting with the point $\mathbf{T}_i$ for the i_{th} iteration, $\mathbf{S}_i$ is found from equation (31) as follows:

$$\mathbf{S}_i = -\frac{\mathbf{P}_i\nabla E(\mathbf{T}_i)}{\|\mathbf{P}_i\nabla E(\mathbf{T}_i)\|} \qquad \#(31)$$

where $\mathbf{P}_i$ represents the projection matrix $\mathbf{P}$ calculated at $\mathbf{T}_i$. If $\mathbf{S}_i = \mathbf{0}$, evaluate the vector λ at the point $\mathbf{T}_i$ as follows:

$$\lambda = -\left(\mathbf{N}^{\mathrm{T}}\mathbf{N}\right)^{-1}\mathbf{N}^{\mathrm{T}}\nabla E(\mathbf{T}_i) \qquad \#(32)$$

Table 2. The gradient projection method of Rosen.

Algorithm 2. The gradient projection method of Rosen [14].

1. Begin with the initial point $\mathbf{T}_1$, at which $c_j(\mathbf{T}_1) \le 0\ \forall j = 1,2,3,\dots,m$.
2. Set i which is the number of iterations as $i = 1$.
3. If $c_j(\mathbf{T}_i) < 0 \forall j = 1,2,3,\dots,m$, set $\mathbf{S}_i = -\nabla E(\mathbf{T}_i)$, normalize it as
   $\mathbf{S}_i = \frac{-\nabla E(\mathbf{T}_i)}{\|\nabla E(\mathbf{T}_i)\|}$ and go to step 5.
   else $\left(c_j(\mathbf{T}_i) = 0\right)$, go to step 5.
4. End if.
5. Evaluate $\mathbf{P}_i$ using the relation $\mathbf{P}_i = \mathbf{I} - \mathbf{N}_r(\mathbf{N}_r^{\mathrm{T}}\mathbf{N}_r)^{-1}\mathbf{N}_r^{\mathrm{T}}$ where
   $\mathbf{N}_r = \left[\nabla c_{j1}(\mathbf{T}_i)\ \nabla c_{j2}(\mathbf{T}_i) \dots \nabla c_{jr}(\mathbf{T}_i)\right]$ then find the normalized search
   direction $\mathbf{S}_i = \frac{-\mathbf{P}_i\nabla E(\mathbf{T}_i)}{\|\mathbf{P}_i\nabla E(\mathbf{T}_i)\|}$.
6. If ($\mathbf{S}_i = \mathbf{0}$), calculate λ at point $\mathbf{T}_i$ using $\lambda = -(\mathbf{N}_r^{\mathrm{T}}\mathbf{N}_r)^{-1}\mathbf{N}_r^{\mathrm{T}}\nabla c(\mathbf{T}_i)$.
   If λ vector has no negative component, take $\mathbf{T}_{\mathrm{opt}} = \mathbf{T}_i$ and stop.
   else find λ_q which is the maximum negative value in λ then form the new
   matrix $\mathbf{N}_{r(\mathrm{new})}$ according to equation (34) and proceed to step 3.
   end if.
   else ($\mathbf{S}_i \neq \mathbf{0}$), find $\lambda_M = \min(\lambda_k), \lambda_k > 0$ which is the the maximum
   step length that violates no constraints and $k \in [1, m]$.
7. End if.
8. Proceed to the next iteration by $\mathbf{T}_{i+1} = \mathbf{T}_i + \lambda_i\mathbf{S}_i$.
9. If $\lambda_M \le \lambda_i^*$ or $\lambda_i = \lambda_M$, there will be some new active constraints at $\mathbf{T}_{i+1}$
   hence compute the new matrix $\mathbf{N}_r$ and go to step 5.
10. End if.
11. If $\lambda_i^* < \lambda_M$ and $\lambda_i = \lambda_i^*$, non of the new constraint become active at $\mathbf{T}_{i+1}$
    hence update the current iteration by $i = i + 1$ and go to step 3.
12. End if.

If the vector λ is positive in all its components, take $\mathbf{T}_{\mathrm{opt}} = \mathbf{T}_i$ and terminate with the current iteration. If λ has some negative components, determine λ_q which is the component with the maximum negative value, then formulate the new matrix $\mathbf{N}_{r(\mathrm{new})}$ by the relation:

$$\mathbf{N}_{r(\mathrm{new})} = \left[\nabla c_{j1}(\mathbf{T}_i) \quad \nabla c_{j2}(\mathbf{T}_i) \dots \nabla c_{jq-1}(\mathbf{T}_i) \quad \nabla c_{jq+1}(\mathbf{T}_i) \dots \nabla c_{jr}(\mathbf{T}_i)\right] \qquad \#(33)$$

by deleting the active constraint ∇c_{jq} corresponding to λ_q and repeating the process. If $\mathbf{S}_i \neq \mathbf{0}$, find λ_M which is the maximum step length by $\lambda_M = \min(\lambda_k), \lambda_k$ is positive and $k \in [1, m]$ then

evaluate $\frac{dE}{d\lambda(\lambda_M)} = \mathbf{S}_i^{\mathrm{T}} \nabla E(\mathbf{T}_i + \lambda_M \mathbf{S}_i)$. If $\frac{dE}{d\lambda(\lambda_M)} \leqslant 0$, then $\lambda_i = \lambda_M$. However, if $\frac{dE}{d\lambda(\lambda_M)} > 0$, use any interpolation method to find the minimizer λ_i^* and take $\lambda_i = \lambda_i^*$. Then the algorithm proceeds to the next iteration by:

$$\mathbf{T}_{i+1} = \mathbf{T}_i + \lambda_i \mathbf{S}_i \qquad \#(34)$$

If $\lambda_M \leq \lambda_i^*$ or if $\lambda_i = \lambda_M$, some constraints may become active at $\mathbf{T}_{i+1}$ so the new matrix $\mathbf{N}_r$ is generated containing the active constraints gradient measured at the new point. If $\lambda_i^* < \lambda_M$ and $\lambda_i = \lambda_i^*$, the matrix $\mathbf{N}_r$ remains unchanged because no constraint become active at $\mathbf{T}_{i+1}$ so the current iteration is updated by $i = i + 1$, and the whole process is repeated. Now the gradient projection method of Rosen could be summarized as shown in algorithm 2.

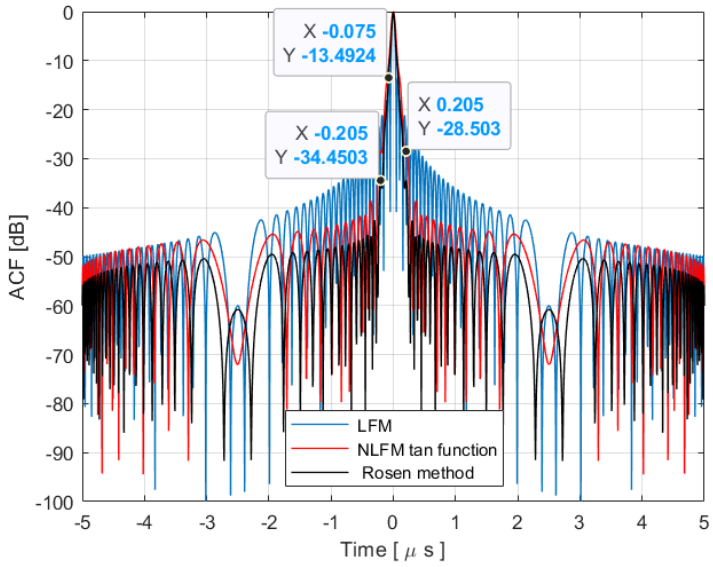

Figure 5. ACF of the signal optimized by Rosen method compared to that of the original non-optimized tan signal and LFM signal.

7. Simulation results of Rosen's method of feasible directions

The ACF of the NLFM signal optimized by the feasible direction method of Rosen is presented in figure 5. As shown, the ACF of the optimized signal has SLL around -34 dB and MLW of 0.0765 μs. This method reduces the SLL by almost 6 dB and enhances the MLW by almost 0.0186 μs compared to the original signal.

8. Discussion

Figure 6 compares both the ACFs of the signal optimized by the proposed techniques to the ACFs of the reference signal and LFM one. This comparison reveals the efficiency of the proposed techniques in suppressing SLL an improving MLW and hence enhancing radar detection capability. As shown in the figure, Zoutendijk's method has a SLL of -40.3437 dB which is lower than the SLL of the LFM signal by almost 27 dB and lower than the SLL of the original signal by 12 dB. On the other hand, Rosen's method has SLL of −34.4503 dB which is lower than that of the LFM signal by 21 dB and lower than that of the non-optimized signal by 6 dB. Furthermore, Zoutendijk's method has narrower MLW than Rosen's method by almost 0.01 μs.

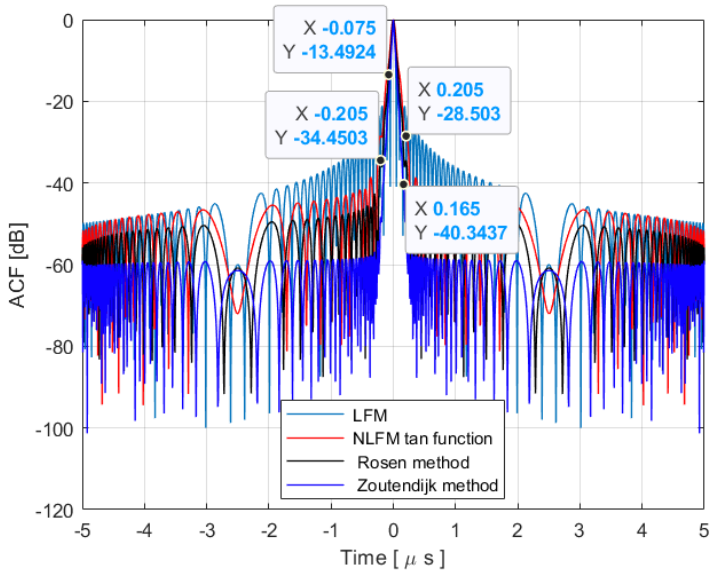

Figure 6. ACFs of the proposed NLFM signal optimized by Zoutendijk and Rosen methods compared to that of the original non-optimized tan signal and LFM signal.

Table 3 summarizes the results of the two techniques compared to the LFM signal and the original non-optimized tan signal. The calculated impulse response width (IRW) and integrated sidelobe ratio (ISLR) of the two techniques are also included in the table compared to the IRW and ISLR of the LFM and the reference tan signal.

Table 3. Comparison between the results of Zoutendijk and Rosen methods.

Algorithm	SLL	MLW*(μs)	IRW	ISLR	Coeff.
LFM	-13.4924 dB	0.0289	1.697 m	−9.69 dB	-
.					$k_1 = 0.1171$
Non-optimized *tan*	-28.5030 dB	0.0951	28.53 m	−24.61 dB	$k_2 = 2.6070$
					$k_1 = 0.1731$
Rosen	−34.4503 dB	0.0765	22.95 m	−29.87 dB	$k_2 = 2.8028$
					$k_1 = 0.2316$
Zoutendijk	−40.3437 dB	0.0673	20.19 m	−35.27 dB	$k_2 = 3.0103$

* Compared to the mainlobe width of LFM signals which is 0.02899 μs.

Table 4. Comparison between the proposed methods and some recent works.

Reference	The used algorithm (optimization technique)	SLL	MLW(μs)
[20]	Firefly algorithm	-34.41 dB	0.0773
[21]	Cyclic algorithm (CA)	-30.12 dB	0.0611
[22]	Invasive weed optimization (IWO)	−22.61 dB	0.0651
Proposed method	Rosen method	−34.45 dB	0.0765
Proposed method	Zoutendijk method	−40.34 dB	0.0673

The complexity is not an issue in this work because it is an offline radar-based application not a real time one. I.e., after getting the coefficients $k_1$and k_2, the operator uses then in the radar signal processor offline not in real time. A comparison between these two techniques and some recent works is shown in table 4.

9. Conclusion and Future Work

In this article, two techniques for optimizing the NLFM signal of tan function have been introduced. The first technique is the feasible direction method of Zoutendijk. The ACF of the signal optimized by this method has SLL of almost -40 dB and MLW of 0.0673 μs i.e., it reduces the SLL of the original signal by 12 dB and enhances the MLW by almost 0.0278 μs. The second technique is the feasible direction method of Rosen which results in an ACF that has SLL around -34 dB and MLW of almost 0.0765 μs. This method suppresses the SLL by almost 6 dB and improves the MLW by 0.0186 μs. The detailed mathematical description of the two proposed approaches is also provided in this paper. Furthermore, a comparison between the results of the four techniques is also provided including the calculated IRW and ISLR of all techniques. As a matter of future work, other optimization techniques such as metaheuristic optimization algorithms that includes particle swarm optimization technique, genetic algorithm, non-Euclidean optimization techniques, and ant colony optimization could be applied together with machine learning-based optimization techniques to the NLFM signal to achieve more enhancements.

10. References

[1] Blunt S D and Mokole E L 2016 Overview of radar waveform diversity *IEEE Aerospace and Electronic Systems Magazine* **31** pp 2-40
[2] Xie Q, Zeng H, and Li W 2022 A Two-Step Optimization Framework for Low Sidelobe NLFM Waveform Using Fourier Series *IEEE Geoscience and Remote Sensing Letters* **19** pp 1-5
[3] Selim M G, Mabrouk G G, Elsherif A K and Youssef A 2023 Effective reduction of sidelobes in pulse compression radars using NLFM signal processing approaches *Journal of Physics: Conf. Series* **2616** p 012034
[4] Ghavamirad R and Sebt M A 2019 Sidelobe level reduction in ACF of NLFM waveform *IET Radar, Sonar and Navigation* **13** pp 74-80
[5] Jin G, Deng Y, Wang R, Wang W, Wang P, Long Y, Zhang Z M and Zhang Y 2019 An Advanced Nonlinear Frequency Modulation Waveform for Radar Imaging with Low Sidelobe *IEEE Transactions on Geoscience and Remote Sensing* **57** pp 6155-6168
[6] Pang C, Hoogeboom P, Le Chevalier F, Russchenberg H W J, Dong J, Wang T and Wang X 2015 A Pulse Compression Waveform for Weather Radars with Solid-State Transmitters *IEEE Geoscience and Remote Sensing Letters* **12** pp 2026-2030
[7] Patrick M and Blunt S D 2017 Nonlinear Conjugate Gradient Optimization of Polyphase-Coded FM Radar Waveforms 2017 *IEEE Radar Conf*. pp 1675-1680
[8] Jin L, Wang J, Zhong Y and Wang D 2022 Optimal Mismatched Filter Design by Combining Convex Optimization with Circular Algorithm *IEEE Access* **10** pp 763-772
[9] Selim M G, Mabrouk G G, Elsherief A K and Youssef A 2023 Nonlinear Optimization Techniques for Radar Signal Enhancement *5th Novel Intelligent and Leading Emerging Sciences Conf., NILES 2023 – Proc.* pp 269-273
[10] Yan J, Ni W, Zhai J and Dong H 2023 An Unambiguity and Anti-Range Eclipse Method for PD Radar Using Biphase Coded Signals *CMES - Computer Modelling in Engineering and Sciences* **134** pp 1337-1351

[11] Das A, Mandal D and Kar R 2020 Side Lobe Suppression of Concentric Circular Antenna Array Using Social Spider Algorithm *IETE J Res* **68** pp 4198-4207
[12] Hussein K F A, Helmy A O and Mohra A S 2022 Radar Pulse Compression with Optimized Weighting Window for SAR Receivers *Wireless Personal Communications* **126** pp 871-893
[13] Devisasi Kala D D and Sundari D T 2023 A review on optimization of antenna array by evolutionary optimization techniques *International Journal of Intelligent Unmanned Systems* **11** pp 151-165
[14] Rao S S 2019 Engineering Optimization: Theory and Practice (New York: *John Wiley & Sons–Interscience) chapter 7* pp 393-407
[15] Alphonse S and Williamson G A 2019 Evaluation of a class of NLFM radar signals *EURASIP Journal on Advances in Signal Processing* **62**
[16] Argenti F and Facheris L 2021 Radar Pulse Compression Methods Based on Nonlinear and Quadratic Optimization *IEEE Transactions on Geoscience and Remote Sensing* **59** pp 904-916
[17] Pagitz M and Pellegrino S 2007 Shape Optimization of "Pumpkin" Balloons *AIAA Balloon Systems Conf.* p 2606
[18] Chen X and Kostreva M M 2000 Methods of Feasible Directions: A Review Progress in Optimization: *Contributions from Australasia* pp 205-219\
[19] Bazaraa M S Sherali H D and Shetty C M 2006 Nonlinear programming: theory and algorithms *John wiley & sons.*
[20] Xu Z, Wang X and Wang Y 2022 Nonlinear Frequency-Modulated Waveforms Modeling and Optimization for Radar Applications *Mathematics* **10**
[21] Jin L, Wang J, Zhong Y and Wang D 2022 Optimal mismatched filter design by combining convex optimization with circular algorithm *IEEE Access* **10** pp 56763-56772.
[22] Devisasi Kala D D and Sundari, D. T. 2023 A review on optimization of antenna array by evolutionary optimization techniques *International Journal of Intelligent Unmanned Systems* **11** pp151-165.